


Research Paper

# ACE2 negatively regulates the Warburg effect and suppresses hepatocellular carcinoma progression via reducing ROS-HIF1 $\alpha$ activity

Fangyuan Dong<sup>1,3,4,5,\*</sup>, Hui Li<sup>2,\*</sup>, Limin Liu<sup>6,\*</sup>, Lin-Li Yao<sup>2,\*</sup>, Jiaofeng Wang<sup>3,4,5</sup>, Danni Xiang<sup>1</sup>, Jianxia Ma<sup>1</sup>, Gansheng Zhang<sup>1</sup>, Shan Zhang<sup>2</sup>, Jun Li<sup>2</sup>, Shu-Heng Jiang<sup>2</sup>, Xiaona Hu<sup>1,3,4,5</sup>, Jie Chen<sup>1,3,4,5</sup>, Zhijun Bao<sup>1,3,4,5</sup>

1. Department of Gastroenterology, Huadong Hospital, Shanghai Medical College, Fudan University, Shanghai 200040, P.R. China.
2. State Key Laboratory of Oncogenes and Related Genes, Shanghai Cancer Institute, Ren Ji Hospital, School of Medicine, Shanghai Jiao Tong University, Shanghai 200240, P.R. China.
3. Shanghai Key Laboratory of Clinical Geriatric Medicine, Shanghai 200040, P.R. China.
4. National Clinical Research Center for Aging and Medicine, Shanghai 200040, P.R. China.
5. Department of Geriatrics, Huadong Hospital, Shanghai Medical College, Fudan University Shanghai 200040, P.R. China.
6. Department of Oral pathology, Ninth People's Hospital, School of Medicine, Shanghai Jiao Tong University, Shanghai 200011, P.R. China.

\*These authors contributed equally to this work.

 Corresponding authors: Prof. Zhijun Bao (zhijunbao@fudan.edu.cn), Prof. Jie Chen (laugh\_chenjie@fudan.edu.cn), Dr. Xiaona Hu (huxnfd@hotmail.com), Department of Gastroenterology, Huadong Hospital, Shanghai Medical College, Fudan University, No.221 Yan'an West Road, Shanghai 200040, P.R. China; or Dr. Shu-Heng Jiang (shjiang@shsci.org), State Key Laboratory of Oncogenes and Related Genes, Shanghai Cancer Institute, Ren Ji Hospital, School of Medicine, Shanghai Jiao Tong University, 800 Dongchuan Road, Shanghai 200240, P.R. China.

© The author(s). This is an open access article distributed under the terms of the Creative Commons Attribution License (<https://creativecommons.org/licenses/by/4.0/>). See <http://ivyspring.com/terms> for full terms and conditions.

Received: 2022.12.03; Accepted: 2023.04.30; Published: 2023.05.11

## Abstract

Aerobic glycolysis has pleiotropic roles in the pathogenesis of hepatocellular carcinoma (HCC). Emerging studies revealed key promoters of aerobic glycolysis, however, little is known about its negative regulators in HCC. In this study, an integrative analysis identifies a repertoire of differentially expressed genes (*DNASE1L3*, *SLC22A1*, *ACE2*, *CES3*, *CCL14*, *GYS2*, *ADH4*, and *CFHR3*) that are inversely associated with the glycolytic phenotype in HCC. *ACE2*, a member of the rennin-angiotensin system, is revealed to be downregulated in HCC and predicts a poor prognosis. *ACE2* overexpression significantly inhibits the glycolytic flux as evidenced by reduced glucose uptake, lactate release, extracellular acidification rate, and the expression of glycolytic genes. Opposite results are noticed in loss-of-function studies. Mechanistically, *ACE2* metabolizes Ang II to Ang-(1-7), which activates Mas receptor and leads to the phosphorylation of Src homology 2-containing inositol phosphatase 2 (SHP-2). SHP2 activation further blocks reactive oxygen species (ROS)-HIF1 $\alpha$  signaling. Addition of Ang-(1-7) or the antioxidant N-acetylcysteine compromises *in vivo* additive tumor growth and aerobic glycolysis induced by *ACE2* knockdown. Moreover, growth advantages afforded by *ACE2* knockdown are largely glycolysis-dependent. In clinical settings, a close link between *ACE2* expression and HIF1 $\alpha$  or the phosphorylated level of SHP2 is found. Overexpression of *ACE2* significantly retards tumor growth in patient-derived xenograft model. Collectively, our findings suggest that *ACE2* is a negative glycolytic regulator, and targeting the *ACE2*/Ang-(1-7)/Mas receptor/ROS/HIF1 $\alpha$  axis may be a promising therapeutic strategy for HCC treatment.

Keywords: Warburg effect; Liver cancer; Hypoxia-inducible factor; Metabolic reprogramming

## Introduction

In normal cells, glycolysis converts glucose to pyruvate, which enters the tricarboxylic acid cycle (TCA) to produce adenosine triphosphate (ATP).

Under pathological conditions such as cancer, fast-growing cancer cells preferentially convert glucose to lactate even in the presence of sufficient

oxygen, a phenomenon termed the Warburg effect or aerobic glycolysis [1-3]. Reprogrammed metabolic reprogramming is widely observed in human cancers such as hepatocellular carcinoma (HCC) and is emerged as a hallmark of cancer [4, 5]. Cancer cells tend to utilize glycolysis rather than oxidative phosphorylation to adapt to the hypoxic tumor microenvironment (TME) and this process largely depends on the abnormally expressed glycolytic genes, such as glucose transporter 1 (GLUT1), hexokinase 2 (HK2), liver-type phosphofructokinase (PFKL), and lactate dehydrogenase A (LDHA) [6-8]. Accumulated studies have revealed a close link between aerobic glycolysis and tumor progression, including but not limited to tumor growth, metastasis, apoptosis, autophagy, stemness, and drug resistance [9]. Notably, tumors with a higher glycolytic capacity are associated with a poorer clinical outcome in HCC patients [10]. Therefore, targeting aerobic glycolysis is a promising strategy and of great importance for cancer treatment.

Previously, many oncogenes have been demonstrated to be key players in the process of aerobic glycolysis, especially hypoxia-inducible factor 1 alpha (HIF1 $\alpha$ ), AKT, c-Myc, FOXK1/2, and SIX1 [10-14]. In HCC, many aberrantly expressed genes are documented as positive glycolysis regulators [15-17]. For instance, PARP14 enhances aerobic glycolysis via inhibition of JNK1-dependent pyruvate kinase M2 (PKM2) phosphorylation and activation [16] and the fatty acid receptor CD36 exerts a stimulatory effect on HCC growth and metastasis in a glycolysis-dependent manner [15]. Recently, we demonstrated that hypoxia-induced MAP17 increases the glycolytic flux of HCC cells via the regulation of reactive oxygen species (ROS) signaling [18]. Although much progress has uncovered the oncogenic drivers of aerobic glycolysis in HCC, the negative regulators of aerobic glycolysis and corresponding molecular mechanisms are incompletely understood. From the therapeutic point of view, pharmacological activation of the negative regulators (tumor suppressors) of glucose metabolism may be an alternate strategy for cancer treatment.

Recently, angiotensin-converting enzyme 2 (ACE2) is known as a host cell receptor for severe acute respiratory syndrome coronavirus 2 (SARS-CoV-2) [19]. As an arm of the renin-angiotensin (Ang) system (RAS), ACE2 can convert angiotensin II (Ang II) to Ang-(1-7), a heptapeptide acting through the Mas receptor [20-22]. The ACE2/Ang(1-7)/Mas receptor axis is frequently downregulated in human cancers and plays tumor-suppressive roles [23-25]. For example, ACE2 inhibits angiogenesis via downregulating the VEGFa/VEGFR2/ERK pathway

in breast cancer [26]. Activation of the ACE2/Ang-(1-7) axis in clear cell renal cell carcinoma (ccRCC) abrogates tumor resistance to VEGFR inhibitors [27]. However, little is known about the link between ACE2 and glycolytic metabolism in cancers.

Given that the positive regulators of aerobic glycolysis are well documented in HCC, we aimed to identify the negative regulators of HCC glycolytic metabolism. In the present study, ACE2 was revealed to be a candidate that is inversely associated with HCC glycolysis. *In vitro* and *in vivo* experiments showed that ACE2 exerts an antitumor effect on HCC via Ang(1-7)/Mas receptor axis. Furthermore, phosphorylation of Src homology 2-containing inositol phosphatase 2 (SHP-2), ROS generation, and HIF1 $\alpha$  signaling were demonstrated to be the functional mediators of ACE2 in HCC.

## Materials and methods

### Cell lines, cell culture, and reagents

HCC cell lines (Huh-7, HCC-LM3, Hep3B, SMMC-7721, SNU-475, MHCC-97L, SK-Hep1, and SUN-389) and the nonmalignant liver cell lines (LO2 and THLE-2) were obtained from the Cell Bank of the Chinese Academy of Sciences (Shanghai, China) or American Type Culture Collection (ATCC; Manassas, VA, USA). Short tandem repeat profiling and mycoplasma contamination examination were done before cell experiments for each cell line. Cells were cultured with Dulbecco's modified Eagle's medium (Gibco, 11965092) or Roswell Park Memorial Institute 1640 medium (Gibco, 11875093), supplemented with 10% fetal bovine serum (FBS, Gibco) and 1% (v/v) streptomycin-penicillin (Sigma-Aldrich, Shanghai, China). All the cells used in this study were cultured in a humidified incubator at 37 °C with 5% CO<sub>2</sub>. The antioxidant N-acetylcysteine (NAC) (S1623), Angiotensin (1-7) (S9820), MLN-4760 (S8940), and Mas receptor inhibitor A-779 (E0039) were all purchased from Selleck (Shanghai, China).

### ACE2 gene expression analysis

The online database TIMER (<https://cistrome.shinyapps.io/timer/>) was employed to investigate the expression profiles of ACE2 across human cancers.

### Prognostic analysis

The online database Kaplan-Meier Plotter (<https://kmplot.com/analysis/>) was used to investigate the prognostic value of ACE2 in HCC. Data were derived from the TCGA cohort and sample grouping was made based on the median mRNA level of ACE2. Kaplan-Meier method was used to determine the prognostic value and the difference was analyzed by

the log-rank test.

### Definition of glycolysis gene signature and sample grouping

A 16-gene expression signature including genes specific to glycolysis (*ALDOA*, *ALDOB*, *ENO1*, *ENO2*, *GAPDH*, *GPI*, *HK2*, *LDHA*, *PFKFB1*, *PFKP*, *PGAM1*, *PGAM2*, *PGK1*, *PKM2*, *SLC2A1*, and *TP11*) was used for the generation of GLYCOLYSIS gene set. Gene set variation analysis (GSVA) was used to calculate the enrichment scores of GLYCOLYSIS gene set based on the expression data set of LIHC from TCGA. The patients were divided into GLYCOLYSIS-high and -low group by the median cutoff of GSVA scoring of GLYCOLYSIS gene set variation analysis. The differentially expressed genes (DEGs) between GLYCOLYSIS-high and -low group were identified using two-tailed Wilcoxon signed rank test and false discovery rate (FDR) correction procedure, and the fold change ( $\log_2FC$ ) between the two groups was calculated.

### Gene set enrichment analysis (GSEA)

The publicly available TCGA-LIHC data was used to characterize the molecular differences in patients with high versus low ACE2 expression. Sample grouping was based on the median value of ACE2 expression, and the sample numbers were sufficient to produce statistically significant differences. GSEA was performed with the Hallmark gene sets. The signaling pathway with a false discovery rate (FDR) less than 0.25 and a P value less than 0.05 were considered significantly enriched.

### Cell transfection

For ACE2 knockdown experiments, two specific short hairpin RNAs (shRNAs) against ACE2 gene were synthesized by GenePharma (Shanghai, China). shRNA plasmids along with a three-plasmid system (pPACKH1-REV, pPACKH1-GAG, and pVSV-G) were transfected into HEK293T cells to generate lentivirus using Lipofectamine 2000 (Invitrogen, Carlsbad, CA, USA) according to the manufacturer's instructions. Lentivirus were collected and subjected to cell infection with polybrene (Sigma-Aldrich, H9268, St. Louis, MO). Stable shRNA-expressing cells were selected with 2  $\mu\text{g}/\text{ml}$  puromycin for 2 weeks. For ACE2 overexpression experiments, the expression construct for human wild type ACE2 (ACE2<sup>WT</sup>) and enzymatic-dead ACE2 (ACE2<sup>H505L</sup>) was synthesized by GenePharma (Shanghai, China) and subcloned into the pGCMV/MCS/IRES/EGFP/Neo plasmid. Stable ACE2-expressing cells were generated by lentivirus infection and the overexpression efficiency was verified by Western blotting.

### Western blotting analysis

Whole-cell proteins were extracted using RIPA lysis buffer (P0013B, Beyotime, Shanghai, China) mixed with protease and phosphatase inhibitor cocktails (ab201119, Abcam, Shanghai, China). The protein concentration was measured by the BCA Protein Assay Kit (Pierce Biotechnology, USA) according to the manufacturer's instructions. The proteins were separated by sodium dodecyl sulfate-polyacrylamide gel electrophoresis and transferred to polyvinylidene difluoride membranes (PVDF; Millipore). The membranes were blocked with 5% bovine serum albumin (BSA) for one hour at room temperature and incubated with primary antibodies at 4 °C overnight. The following antibodies were used in this study: ACE2 (1:1000, Abcam, ab108252), HIF1 $\alpha$  (1: 1000, Abcam, ab113642), p-P38 (1:1000, Cell Signaling Technology, #4511), P38 (1:1000, Cell Signaling Technology, #8690), p-p44/42 MAPK (1:1000, Cell Signaling Technology, #4370), p44/42 MAPK (1:2,000, Cell Signaling Technology, #4695), p-JNK (1:1000, Cell Signaling Technology, #9255), JNK (1:2,000, Cell Signaling Technology, #9252), p-P65 (1:1,000, Cell Signaling Technology, #3033), P65 (1:1000, Cell Signaling Technology, #8242), p-Akt (1:2,000, Cell Signaling Technology, #4060), Akt (1:1000, Cell Signaling Technology, #4685), p-SHP2 (1:1,000, Cell Signaling Technology, #5431), SHP2 (1:1000, Cell Signaling Technology, #3397), and  $\beta$ -actin (1:2000, Abcam, ab8226). On the second day, the membranes were incubated with HRP-conjugated secondary antibodies for 45 min at room temperature and visualized using an ECL chemiluminescence assay.

### Quantitative real-time PCR (qRT-PCR)

Total RNA was extracted from indicated HCC cell lines or xenograft tumor tissues using the RNAiso Plus reagent (Takara, Japan) and subjected to reverse transcription reaction using the PrimeScript RT-PCR kit (Takara, Japan). qRT-PCR was performed with SYBR Green (Takara, Japan) on a 7500 Real-time PCR system (Applied Biosystems, Inc. USA). The housekeeping gene ACTB was used as an internal control. The sequences of primers were shown as follows: ACE2 forward, 5'-CAAGAGCAAACGGTTG AACAC-3'; ACE2 reverse 5'-CCAGAGCCTCTCATT GTAGTCT-3'; SLC2A1 forward, 5'-ATTGGCTCCGGT ATCGTCAAC-3'; SLC2A1 reverse, 5'-GCTCAGATAG GACATCCAGGGTA-3'; HK2 forward, 5'-TTGACCA GGAGATTGACATGGG-3'; HK2 reverse, 5'-CAAC CGCATCAGGACCTCA-3'; ENO1 forward, 5'-TGG TGCTATCGAAGATCCCTT-3'; ENO1 reverse, 5'-CCTTGGCGATCCTCTTTGG-3'; PFKL forward, 5'-GCTGGCGGCACTATCATT-3'; PFKL reverse,



5'-TCAGGTGCGAGTAGGTCCG-3'; LDHA forward, 5'-ATGGCAACTCTAAAGGATCAGC-3'; LDHA reverse, 5'-CCAACCCCAACAACCTGTAATCT-3'; PDK1 forward, 5'-GGATTGCCATATCACGCTTT-3'; PDK1 reverse, 5'-TCCCGTAACCCTCTAGGGAATA-3'; ACTB forward, 5'-ACTCGTCATCTCCTGCT-3', ACTB reverse, 5'-GAAACTACCTTCAACTCC-3'.

### Measurement of glucose and lactate level

Glucose and lactate levels in the cell supernatant were detected as reported previously [29]. The Amplex Red Glucose/Glucose Oxidase Assay Kit (A22189, Thermo Fisher Scientific, USA) and the Lactate Assay Kit (K607-100, BioVision, USA) were used to detect glucose and lactate levels, respectively. The acquired data were further normalized to the corresponding protein concentration of cell extracts. All the experiments were run in triplicate and repeated at least two times.

### Extracellular acidification rate (ECAR)

The Seahorse Bioscience XF96 Extracellular Flux Analyzer (Seahorse Bioscience, USA) was used to analyze ECAR in HCC cells upon different treatments. ECAR measurement was analyzed with Seahorse XF Cell Glycolysis Stress Test Kit (Seahorse Bioscience, USA) according to the manufacturer's protocols. In this study, 10 mM glucose, 0.5-1  $\mu$ M oligomycin (Oligo), and 80 mM 2-deoxyglucose (2-DG) were used for ECAR detection. The acquired data were further normalized to the corresponding protein concentration of cell extracts.

### HIF1 $\alpha$ transcriptional activity

The commercial HIF1 $\alpha$  Transcription Factor Assay Kit (ab133104, Abcam) was used to determine the effect of ACE2/Mas receptor/NAC on HIF1 $\alpha$  activity. In brief, nuclear extract lysates were harvested from indicated HCC cells by using a Nuclear Extraction Kit (#2900, Millipore), followed by HIF1 $\alpha$  activity detection with the assay kit according to the manufacturer's protocols.

### Detection of reactive oxygen species (ROS)

For evaluating the level of cellular ROS,  $1 \times 10^4$  indicated HCC cells were seeded at a well of black 96-well plates and subjected to DCF-DA (10 mmol/L) staining in phenol red-free medium for 30 min at room temperature. Then the fluorescence intensity was detected immediately using a BioTek FLx800 Microplate Fluorescence Readers.

### Cell proliferation assay

HCC cells were seeded at 500 cells per well in 6-well plates. The culture medium was replaced every

2-3 days and cells were cultured for 10-14 days. At the end time point, HCC cells were fixed with 4% paraformaldehyde for 15 min and stained with 0.1% crystal violet for 20 min. After washing with PBS three times, the colonies were counted. All the experiments were run in triplicate and repeated at least two times.

### Cell apoptosis assay

The commercial Apo-ONE Homogeneous Caspase-3/7 Assay Kit (Promega, G7790, USA) was used to determine cell apoptosis. CellTiter-Blue (Promega, G8081) was used to evaluate cell numbers. At the endpoint of experiments, cell number and caspase-3/7 activity were monitored in the same sample. The Caspase-3/7 activity was calculated as the ratio of Apo-ONE/CellTiter-Blue signals according to the manufacturer's instructions. All the experiments were run in triplicate and repeated at least two times.

### Animal experiments

Male BALB/c nude mice aged six to eight weeks were purchased from Shanghai Jiesijie Laboratory Animal Technology Company. Mice were housed in pathogen-free conditions and maintained in a 12/12 h light-dark cycle with free access to standard food and tap water. To generate a subcutaneous xenograft model,  $2 \times 10^6$  indicated HCC cells were resuspended in 100  $\mu$ L PBS and then implanted into the flanks of mice. The volume of xenograft tumors was monitored every 3 or 4 days. For patient-derived xenograft (PDX) model, two HCC samples were acquired and subjected for evaluation of ACE2 expression. For treatment of AAV (GenePharma, Shanghai, China), tumor-bearing mice were intratumorally injected with control AAV or AAV-oeACE2. Tumor volume was estimated as follows: tumor volume = length $\times$ width<sup>2</sup>/2. At the endpoint of the animal experiment, the mice were sacrificed and the xenograft tumors were isolated and weighed. This study was approved by the Research Ethics Committee of Huadong Hospital, Shanghai Medical College, Fudan University and carried out following the guidelines of the national animal protection and ethics institute.

### Immunohistochemistry

A microarray containing 202 matched HCC and nontumor tissues was used as reported previously [28]. Immunohistochemical (IHC) analysis was carried out as reported previously [29]. The following primary antibodies were used for IHC analysis: ACE2 (1:200, Abcam, ab108252), Ki67 (1:400, Cell Signaling Technology, #9449), cleaved caspase 3 (1:400, Cell Signaling Technology, #9661), HIF1 $\alpha$  (1:200, Abcam, ab51608), and p-SHP2 (1:200, Abcam, ab75818).



Scoring was conducted based on the percentage of positive staining cells and staining intensity as reported previously [30]. “-” indicates no staining, “+” indicates weak staining, “++” indicates moderate staining, and “+++” indicates strong staining. “-” and “+” were defined as low ACE2 expression, while “++” and “+++” were defined as high ACE2 expression.

### Statistical analysis

All the data were presented as means  $\pm$  SEM from at least three independent experiments. When comparing two independent groups, a two-tailed Student's t-test was used. When comparing two independent groups. Statistical analyses for more than two groups (parametric variables) were performed with a two-way analysis of variance (ANOVA) followed by post hoc Duncan tests. GraphPad Prism (GraphPad Software Inc., San Diego, CA) was used for statistical analyses. P-value less than 0.05 was considered statistically significant.

## Results

### Identification of negative regulators of aerobic glycolysis in HCC

To decipher the potential negative regulators of HCC glycolysis, we leveraged the molecular profiles of Liver hepatocellular carcinoma (LIHC,  $n = 371$ ) from the TCGA cohort (Figure 1A). Based on a 16-gene expression signature including genes specific to glycolysis, we divided the LIHC samples into two groups (glycolysis-high vs. glycolysis-low) and identified 605 differentially expressed protein-coding genes (DEGs) that negatively associated with glycolysis (Supplementary Table 1). Among these DEGs, several top hits (*SLC10A1*, *CYP3A4*, *SPP2*, and *LECT2*) were also revealed to be negative glycolytic regulators in HCC by other group [31], indicating that our analysis was built on the meaningful context of aerobic glycolysis. Moreover, 501 prognosis-associated genes and 721 differentially expressed and downregulated genes were found in HCC. By merging genes from the above three lists, we identified 8 candidates (*DNASE1L3*, *SLC22A1*, *ACE2*, *CES3*, *CCL14*, *GYS2*, *ADH4*, and *CFHR3*) (Figure 1B). Notably, *DNASE1L3* has been reported to inhibit HCC progression by inducing cell apoptosis and weakening tumor glycolysis [32]. *SLC22A1* is downregulated in HCC and may affect the response to sorafenib [33]. A preventive role of *CES3* protein has been reported in the early stages of liver cancer development [34]. *CCL14* suppresses cell proliferation and promotes cell apoptosis in HCC [35]. *GYS2* functions as a tumor suppressor in HCC via regulation of p53 activity [36], and *ADH4* serves as a

prognostic marker in HCC [37]. *CFHR3* is a novel prognostic biomarker for HCC [38]. Given the known roles of these seven candidates, we focused on *ACE2*, which is poorly studied in HCC. Based on the expression level of *ACE2*, we performed gene set enrichment analysis (GSEA) and the result revealed that *ACE2* was significantly and inversely associated with the glycolysis gene signature (Figure 1C). Downregulation of *ACE2* was noticed in several cancer types, including HCC (Figure 1D). Additionally, compared to patients with lower *ACE2* expression, patients with higher *ACE2* expression had significantly improved overall survival (HR = 0.54; 95% CI, 0.38-0.76;  $P = 4e-04$ ) (Figure 1E) and disease-free survival (HR = 0.44; 95% CI, 0.28-0.68;  $P = 2e-04$ ) (Figure 1F). Immunofluorescence analysis showed the positive staining of *ACE2* was mostly membrane and cytoplasmic staining (Figure 1G). To further address the prognostic value of *ACE2* in HCC, immunohistochemical analysis of *ACE2* expression in an HCC tissue microarray (Ren Ji cohort) was performed. As a result, *ACE2* expression was downregulated in HCC tissues compared with corresponding normal liver tissues (Figure 1H). Consistently, higher *ACE2* expression predicted a better prognosis in HCC patients (Figure 1I). Collectively, these findings suggest that a close connection between *ACE2* and aerobic glycolysis in HCC.

### ACE2 is a negative regulator of aerobic glycolysis in HCC

To investigate whether *ACE2* can inhibit HCC glycolysis or not, both gain-of-function and loss-of-function experiments were performed. Firstly, Western blotting was carried out to evaluate the protein level of *ACE2* in HCC cell lines. Compared with the nonmalignant LO2 and THLE-2 cell lines, *ACE2* was less expressed in HCC cell lines (Figure 2A). Then, two cell lines, SNU-475 and SK-Hep1, with lower *ACE2* expression, were selected for the gain-of-function study (Figure 2B). It is worth mentioning that SK-Hep-1 is a cell line isolated from the ascitic fluid of a patient with liver adenocarcinoma and has been identified as being of endothelial origin [39]. To measure the changes in the glycolytic flux, we detected glucose uptake, lactate release, extracellular acidification rate (ECAR), and the mRNA level of glycolytic genes after *ACE2* overexpression. In SNU-475 and SK-Hep1 cells, *ACE2* overexpression led to a remarkable reduction in glucose uptake (Figure 2C), lactate release (Figure 2D), ECAR (Figure 2E), and expression of glucose transporter (*SLC2A1*) and glycolytic genes (*SLC2A1*, *HK2*, *ENO1*, *PFKL*, *LDHA*, and *PDK1*) (Supplementary Figure 1A). Moreover,

loss-of-function experiments were done in HCC-LM3 and Hep3B cells. Two shRNAs against ACE2 resulted in marked downregulation in the ACE2 protein level (Figure 2F). In contrast to ACE2 overexpression, ACE2 knockdown promoted glucose uptake (Figure 2G), lactate release (Figure 2H), ECAR (Figure 2I), and expression of glycolytic components (Supplementary Figure 1B) in HCC-LM3 and Hep3B cells. Moreover, inhibition of ACE2 with 5 μM MLN-4760 phenocopied the glycolysis-promoting effects of

ACE2 knockdown in HCC cells (Figure 2J-L). To rule out the decrease of glucose metabolism may be a direct effect from impairing cellular growth, we further checked the glucose uptake and lactate production at 12 h, at which time cellular growth remained unaffected. As a result, the effects of ACE2 on HCC glucose metabolism were still existed (Supplementary Figure 2). Taken together, ACE2 is evidently involved in the regulation of glycolytic metabolism.

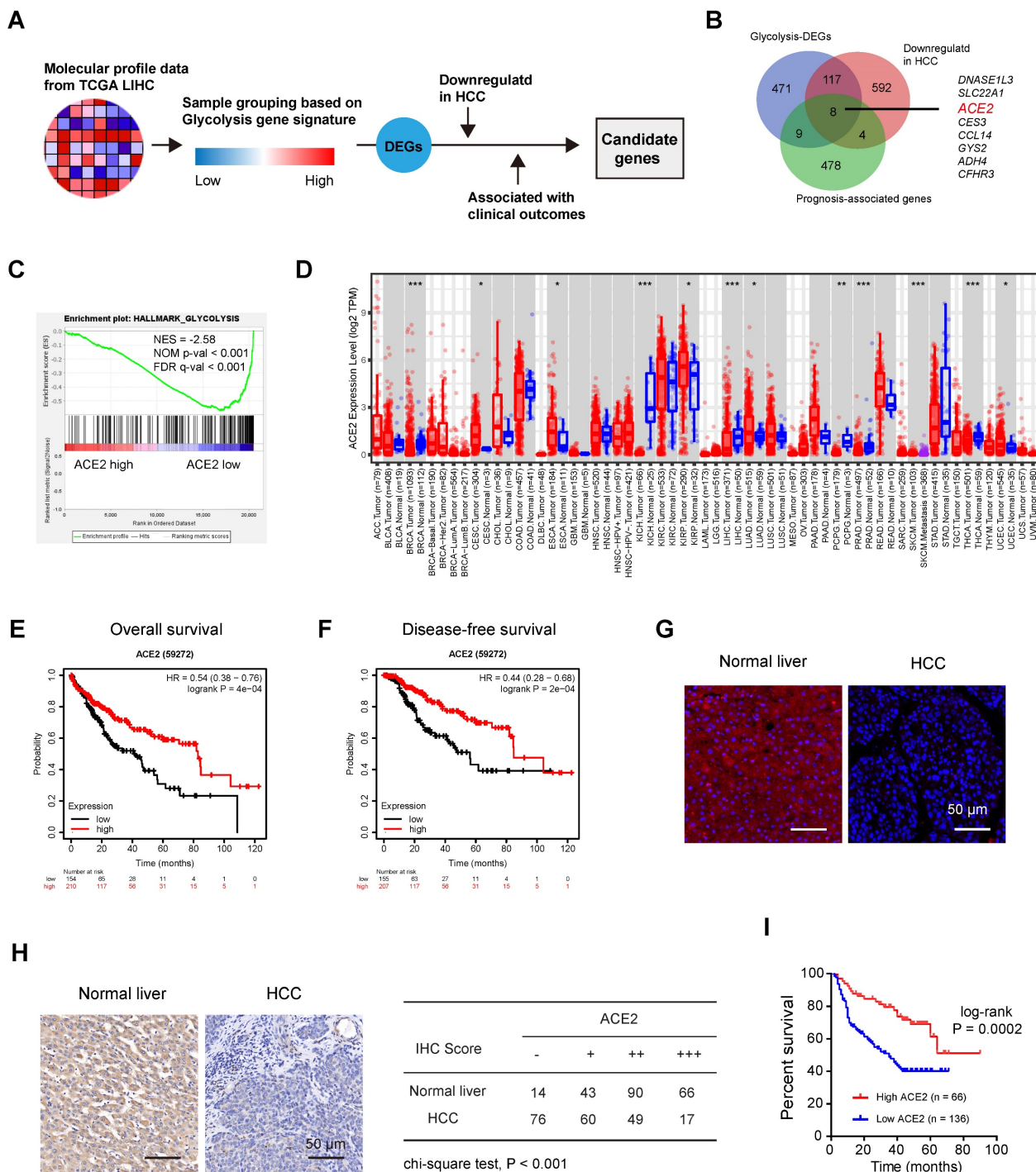


**Figure 1.** Identification of negative regulators of aerobic glycolysis in HCC. (A) Workflow for identifying differentially expressed genes (DEGs) related to glycolysis in HCC. (B) Genes that negatively linked to glycolysis, genes that downregulated in HCC, and prognosis-associated genes were merged. All the differentially expressed genes

(DEGs) were identified with The Cancer Genome Atlas (TCGA) cohort. (C) Gene set enrichment analysis (GSEA) of ACE2-based gene expression patterns with the hallmark glycolysis gene set. (D) The expression profile of ACE2 across human cancers; data were derived from the TIMER database. (E) Kaplan-Meier curve analysis for overall survival in HCC patients (TCGA cohort) based on the median expression value of ACE2 expression; HR: hazard ratio. (F) Kaplan-Meier curve analysis for disease-free survival in HCC patients (TCGA cohort) based on the median expression value of ACE2 expression; HR: hazard ratio. (G) Immunofluorescence analysis showed ACE2 signals in human normal liver and HCC; scale bar, 50  $\mu$ m. (H) Representative images of ACE2 expression in HCC tissues and corresponding normal liver tissues. "-" indicates no staining, "+" indicates weak staining, "++" indicates moderate staining, and "+++" indicates strong staining. "-" and "+" were defined as low ACE2 expression, while "++" and "+++" were defined as high ACE2 expression. (I) Kaplan-Meier curve analysis for overall survival in HCC patients based on the IHC results of ACE2 staining in Ren Ji cohort (n = 202). ACC, Adrenocortical carcinoma; BLCA, Bladder urothelial carcinoma; BRCA, Breast invasive carcinoma; CESC, Cervical squamous cell carcinoma and endocervical adenocarcinoma; CHOL, Cholangio carcinoma; COAD, Colon adenocarcinoma; DLBC, Lymphoid neoplasm diffuse large B-cell lymphoma; ESCA, Esophageal carcinoma; GBM, Glioblastoma multiforme; HNSC, Head and neck squamous cell carcinoma; KICH, Kidney chromophobe; KIRC, Kidney renal clear cell carcinoma; KIRP, Kidney renal papillary cell carcinoma; LAML, Acute myeloid leukemia; LGG, Brain lower grade glioma; LIHC, Liver hepatocellular carcinoma; LUAD, Lung adenocarcinoma; LUSC, Lung squamous cell carcinoma; MESO, Mesothelioma; OV, Ovarian serous cystadenocarcinoma; PAAD, Pancreatic adenocarcinoma; PCPG, Pheochromocytoma and paraganglioma; PRAD, Prostate adenocarcinoma; READ, Rectum adenocarcinoma; SARC, Sarcoma; SKCM, Skin cutaneous melanoma; STAD, Stomach adenocarcinoma; TGCT, Testicular germ cell tumors; THCA, Thyroid carcinoma; THYM, Thymoma; UCEC, Uterine corpus endometrial carcinoma; UCS, Uterine carcinosarcoma; UVM, Uveal melanoma. \*P < 0.05; \*\*P < 0.01; \*\*\*P < 0.001.

### ACE2 depends on the Ang-(1-7)/Mas receptor axis to inhibit aerobic glycolysis

ACE2 cleaves Ang II to generate Ang-(1-7), which further activates Mas receptor to initiate a downstream signaling cascade (Figure 3A). To determine whether this is the case, we verified the roles of ACE2 on HCC glycolysis in the presence or absence of Ang-(1-7) and the Mas receptor inhibitor A779 [40]. As displayed in Figure 3B-D, the addition of 1  $\mu$ M A779 restored the decrease in glucose uptake, lactate release, and ECAR induced by ACE2 overexpression. Moreover, we added Ang-(1-7) ( $10^{-8}$  M) to the culture medium of ACE2 knockdown cells. Expectedly, increased glycolytic capacity observed in ACE2 knockdown cells was largely compromised by Ang-(1-7) treatment as evidenced by the reduced level of glucose uptake, lactate release, and ECAR (Figure 3E-G). To further test whether enzymatic activity of ACE2 is required for its regulatory role in glycolysis, we transfected SNU-475 cells with ACE2 catalytic site histidine mutation (H505L) (Figure 3H). Compared with wild type ACE2, enzymatic-dead ACE2 failed to suppress glycolysis as revealed by glucose uptake, lactate release, and ECAR (Figure 3I-K). Taken together, the enzymatic activity of ACE2 and Mas receptor are needed for the inhibitory roles of ACE2 on HCC glycolysis.

### ACE2 suppresses HIF1 $\alpha$ activity in HCC

Next, we aimed to delineate the underlying molecular mechanism responsible for ACE2-mediated glycolytic changes. As analyzed above, we also identified other molecular differences in the molecular profile data associated with ACE2 expression. As a result, significant enrichment in hypoxia signaling was observed (Figure 4A). Given that HIF1 $\alpha$  is a key transcriptional factor for glycolytic metabolism [14], we, therefore, investigated the link between ACE2 and HIF1 $\alpha$ . Using a commercial detection kit, we first detected HIF1 $\alpha$  transcriptional activity upon ACE2 overexpression. Intriguingly,

HIF1 $\alpha$  transcriptional activity was markedly attenuated by ACE2 overexpression and can be further rescued by the addition of A779 (Figure 4B). In contrast, ACE2 knockdown increased HIF1 $\alpha$  transcriptional activity, which can also be blocked by the addition of Ang-(1-7) (Figure 4C). Previously, several known downstream signaling molecules of Mas receptor have been revealed, such as MAPKs (p38, ERK1/2, JNK), NF- $\kappa$ B, and AKT [41]. Moreover, Ang-(1-7) can counterbalance Ang II signaling via hijacking Ang II-induced SHP-2 dephosphorylation and reactive oxygen species (ROS) generation [42]. By Western blotting analysis, we observed that ACE2 overexpression significantly increased the phosphorylated level of SHP2 and decreased HIF1 $\alpha$  activity, but had no significant implications on MAPKs, NF- $\kappa$ B, and AKT signaling in SNU-475 and SK-Hep1 cells (Figure 4D). Conversely, ACE2 knockdown suppressed SHP2 phosphorylation and increased the HIF1 $\alpha$  level (Figure 4E), indicating that ACE2 might modulate SHP2 phosphorylation to influence the HIF1 $\alpha$  level. To further determine whether ROS is essential for ACE2-dependent HIF1 $\alpha$  activity, we detected ROS levels upon manipulation of the ACE2/Ang-(1-7)/Mas receptor. As shown in Figure 4F, ACE2 overexpression reduced ROS level, and inhibition of Mas receptor with A779 rescued ROS level. In opposite, ACE2 knockdown increased ROS level, and the addition of Ang-(1-7) further blocked ROS generation (Figure 4G). To elucidate whether ROS is responsible for ACE2-dependent HIF1 $\alpha$  activity in HCC, we blocked ROS function with the addition of the antioxidant N-acetylcysteine (NAC). Indeed, increased HIF1 $\alpha$  transcriptional activity induced by ACE2 knockdown was blocked by NAC (Figure 4H). Likewise, NAC also blocked the increased glucose uptake, lactate release, and ECAR induced by ACE2 knockdown in HCC-LM3 and Hep3B cells (Supplementary Figure 3). Collectively, ACE2 may inhibit ROS generation to regulate HIF1 $\alpha$  activity and aerobic glycolysis in HCC.



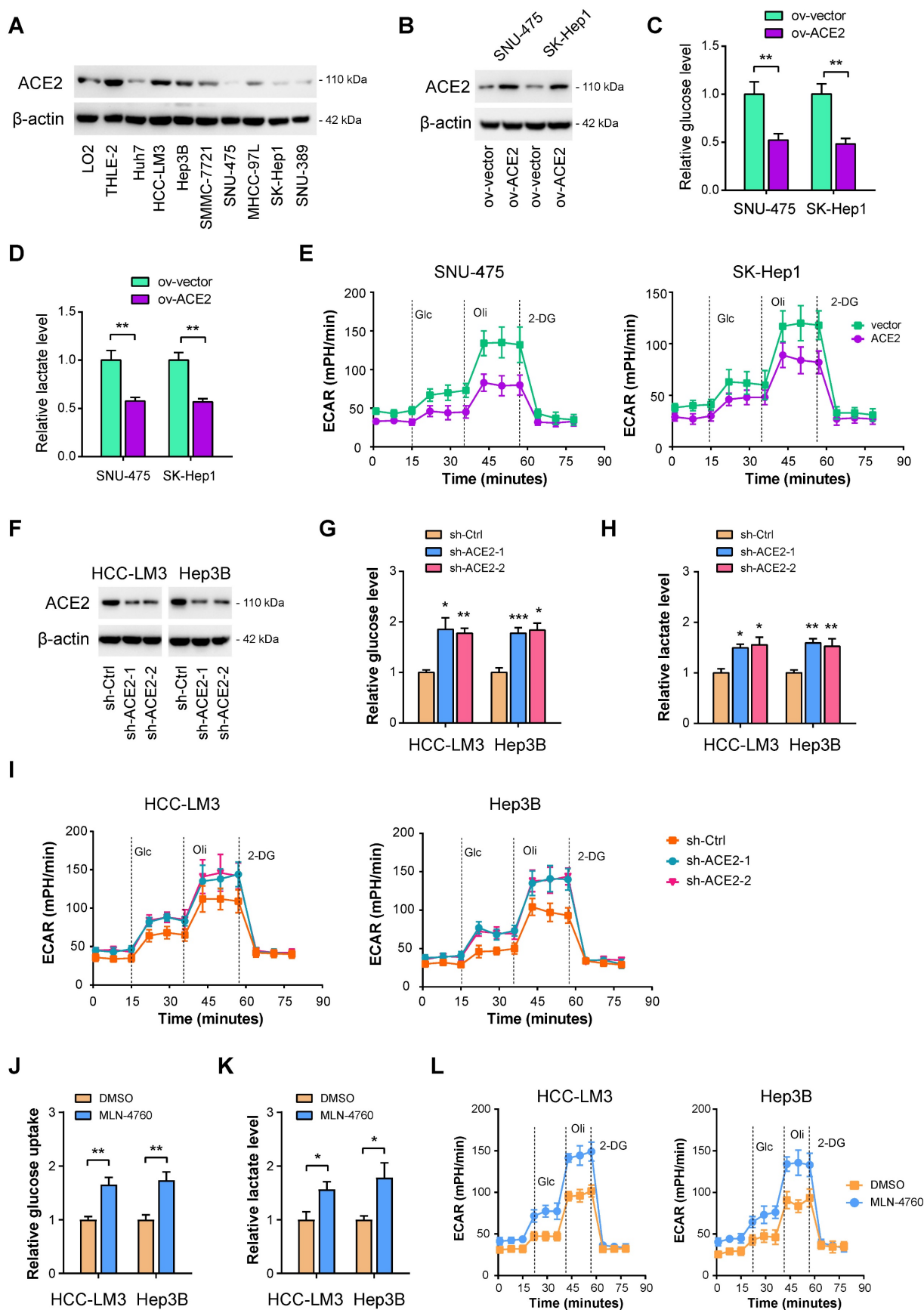


**Figure 2. ACE2 is a negative regulator of aerobic glycolysis in HCC.** (A) The protein levels of ACE2 in liver cancer cells and the nonmalignant cells (LO2 and THLE-2) were verified by Western blotting. (B) The overexpression efficiency of ACE2 in SNU-475 and SK-Hep1 cells was tested by Western blotting analysis. (C-E) The influences of ACE2 overexpression on the glucose uptake (C, n = 3), lactate release (D, n = 3), and extracellular acidification rate (E, n = 3) in SNU-475 and SK-Hep1 cells. (F) Two independent shRNAs against ACE2 were used for knockdown of ACE2 and the knockdown efficiency was verified by Western blotting in HCC-LM3 and Hep3B cells. (G-I) The

influences of ACE2 knockdown on the glucose uptake (G, n = 3), lactate release (H, n = 3), and extracellular acidification rate (I, n = 3) in HCC-LM3 and Hep3B cells. (J-L) The influences of ACE2 inhibitor MLN-4760 (5 μM) on the glucose uptake (J, n = 3), lactate release (K, n = 3), and extracellular acidification rate (L, n = 3) in HCC-LM3 and Hep3B cells. \*P < 0.05; \*\*P < 0.01; \*\*\*P < 0.001.

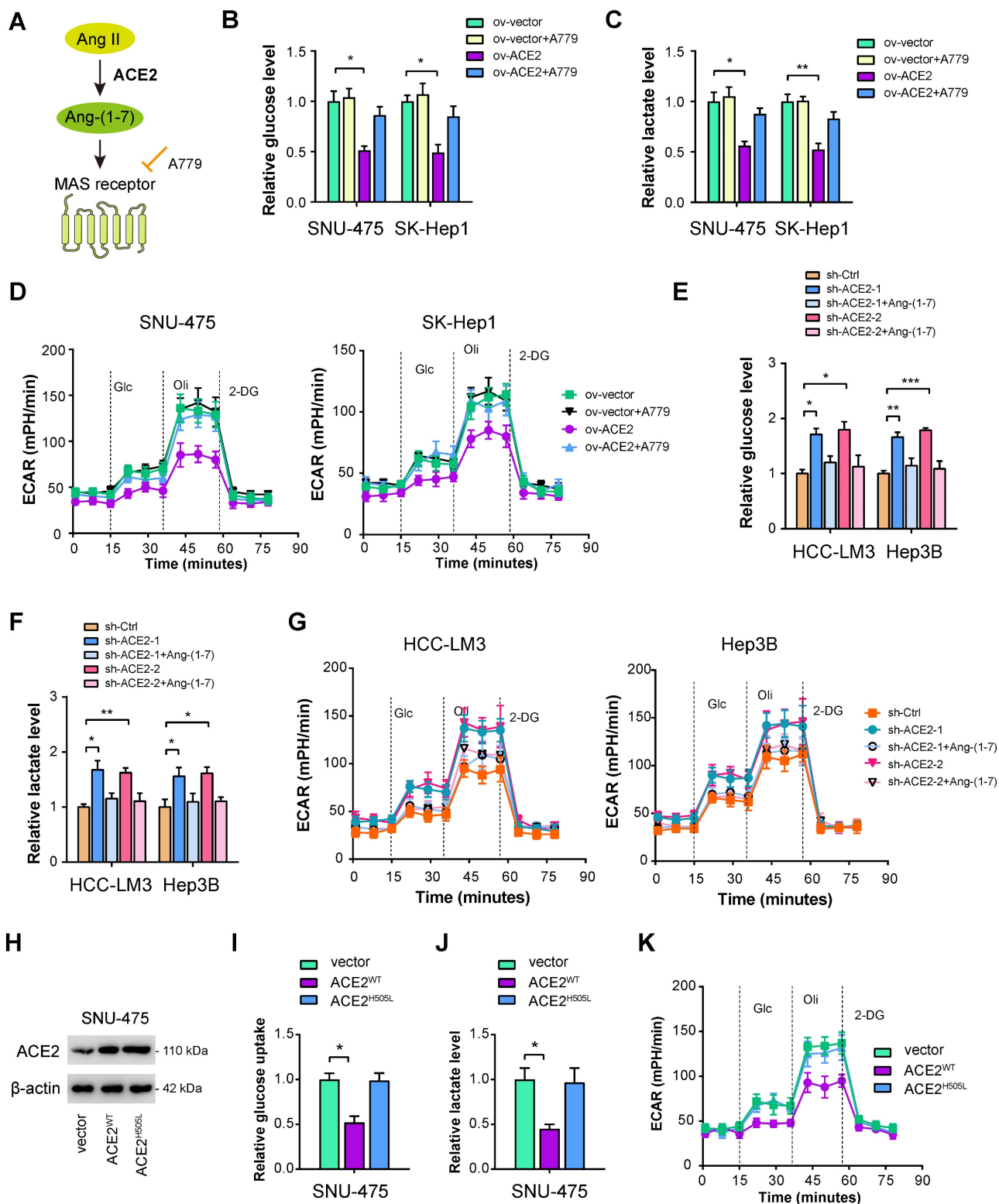


**Figure 3. ACE2 depends on the Ang-(1-7)/Mas receptor axis to inhibit aerobic glycolysis.** (A) Simplified view of the ACE2/Ang-(1-7)/Mas receptor axis. (B-D) The effects of ACE2 overexpression on the glucose uptake (B, n = 3), lactate release (C, n = 3), and extracellular acidification rate (D, n = 3) in the presence or absence of A779 (1 μM) were measured in SNU-475 and SK-Hep1 cells. (E-G) The influences of ACE2 knockdown on the glucose uptake (E, n = 3), lactate release (F, n = 3), and extracellular acidification rate (G, n = 3) in the presence or absence of Ang-(1-7) (10<sup>-8</sup> M) were detected in HCC-LM3 and Hep3B cells. (H) The overexpression efficiency of wild type ACE2 (ACE2<sup>WT</sup>) and enzymatic-dead ACE2 (ACE2<sup>H505L</sup>) in SNU-475 cells was tested by Western blotting analysis. (I-K) The influences of ACE2<sup>WT</sup> and ACE2<sup>H505L</sup> on the glucose uptake (I, n = 3), lactate release (J, n = 3), and extracellular acidification rate (K, n = 3) in SNU-475 cells. \*P < 0.05; \*\*P < 0.01; \*\*\*P < 0.001.

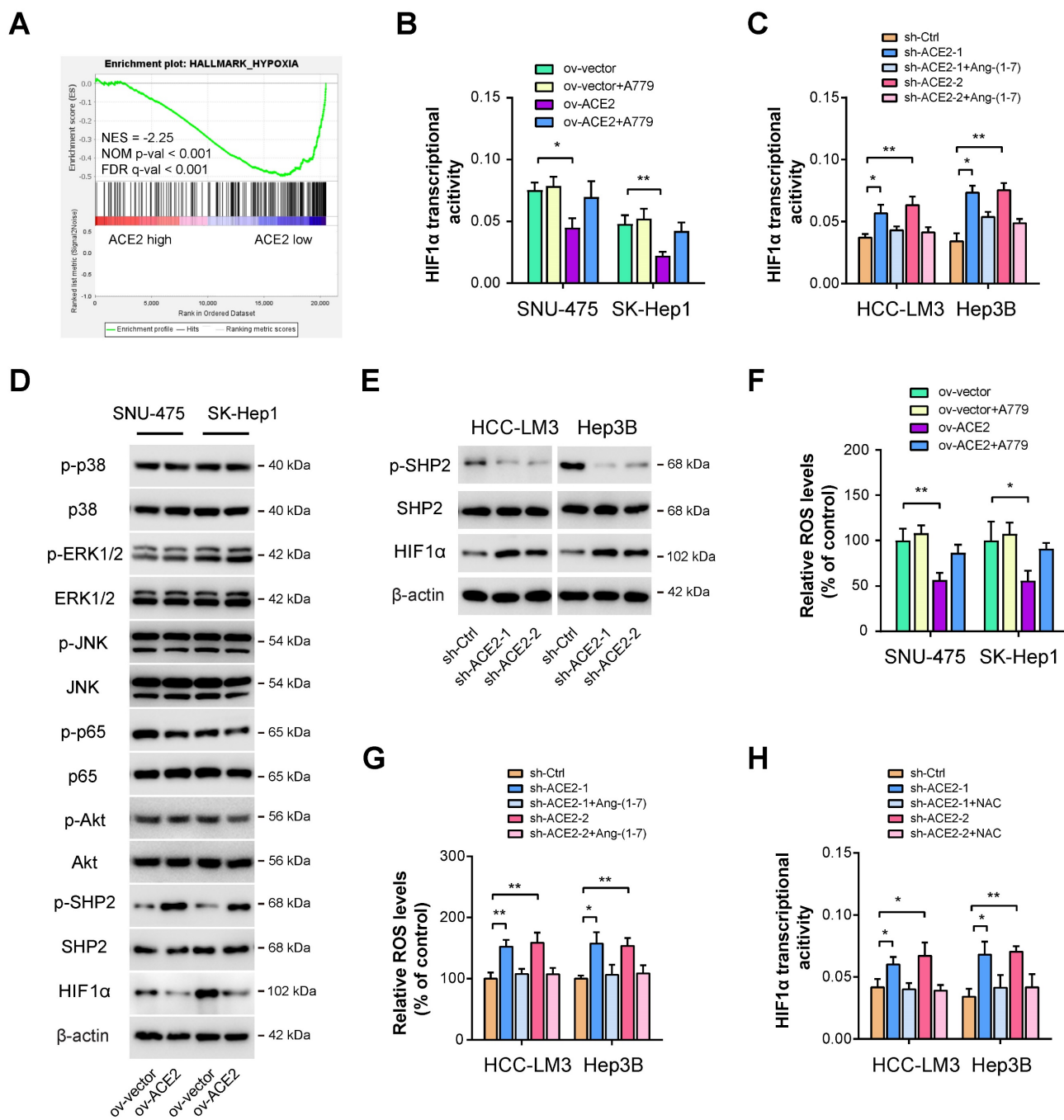


**Figure 4. ACE2 suppresses HIF1α activity in HCC.** (A) GSEA plot showed a close link between ACE2 expression and hypoxia in HCC samples from the TCGA cohort. (B) The effects of ACE2 overexpression on HIF1α transcriptional activity in the presence or absence of A779 (1 μM) were measured in SNU-475 and SK-Hep1 cells. (C) The effects of ACE2 knockdown on HIF1α transcriptional activity in the presence or absence of Ang-(1-7) (10<sup>-8</sup> M) were measured in HCC-LM3 and Hep3B cells. (D) The effects of ACE2 overexpression on the activity of ACE2-associated signaling pathways (p38 MAPK, ERK1/2, JNK, NF-κB, AKT, SHP2, and HIF1α) in SNU-475 and SK-Hep1 cells was analyzed by Western blotting. (E) The levels of p-SHP2, SHP2, and HIF1α in sh-Ctrl and sh-ACE2 HCC-LM3 and Hep3B cells was analyzed by Western blotting. (F) The effects of ACE2 overexpression on ROS generation in the presence or absence of A779 (1 μM) were measured in SNU-475 and SK-Hep1 cells. (G) The effects of ACE2 knockdown on ROS generation in the presence or absence of Ang-(1-7) (10<sup>-8</sup> M) were measured in HCC-LM3 and Hep3B cells. (H) The effects of ACE2 knockdown on HIF1α transcriptional activity in the presence or absence of 1 mM N-acetyl cysteine (NAC) treatment were measured in HCC-LM3 and Hep3B cells. \*P < 0.05 and \*\*P < 0.01.

### ACE2 overexpression inhibits HCC tumor growth

To answer whether ACE2 plays tumor-suppressive roles in HCC, we performed *in vitro* and *in vivo* experiments. Plate colony formation assay showed that ACE2 overexpression reduced *in vitro* cell proliferation of SNU-475 and SK-Hep1 cells and the

inhibitory roles of ACE2 on cell proliferation can be restored by A779 (Figure 5A). Furthermore, we generated a subcutaneous xenograft model by implanting SK-Hep1 cells into the flanks of immunocompromised mice. The result showed that ACE2 overexpression retarded tumor growth, while A779 blocked the effect of ACE2 overexpression



(Figure 5B). In another cohort of animal experiments, mice in the ov-ACE2 group had improved survival compared with mice in the ov-vector or ov-ACE2 + A779 group (Figure 5C). The inhibitory effect of the ACE2/Mas receptor axis was further supported by IHC analysis of the proliferation index Ki-67. Notably, cell apoptosis was not induced by genetic manipulation of ACE2, either overexpression or knockdown, as demonstrated by the IHC staining of cleaved caspase 3 (CCS3) and *in vitro* caspase-3/7 activity (Figure 5D and Supplementary Figure 4). Real-time qPCR analysis of glucose transporter and glycolytic genes in the xenograft tumor tissues showed that ACE2 overexpression suppressed the mRNA levels of SLC2A1, HK2, ENO1, PFKL, LDHA,

and PDK1, while inhibition of Mas receptor with A779 restored the expression of glycolytic components (Figure 5E).

### ACE2 knockdown promotes HCC tumor growth

To further strengthen the inhibitory effect of ACE2 on tumor growth, we performed a loss-of-function experiment in HCC-LM3 and Hep3B cells. Plate colony formation showed that ACE2 knockdown promoted the *in vitro* proliferation of HCC-LM3 and Hep3B cells, but had no significant effects on cell apoptosis as indicated by Caspase-3/7 activity (Figure 6A). *In vivo* studies showed that tumors formed by sh-ACE2-1 HCC-LM3 cells grew more

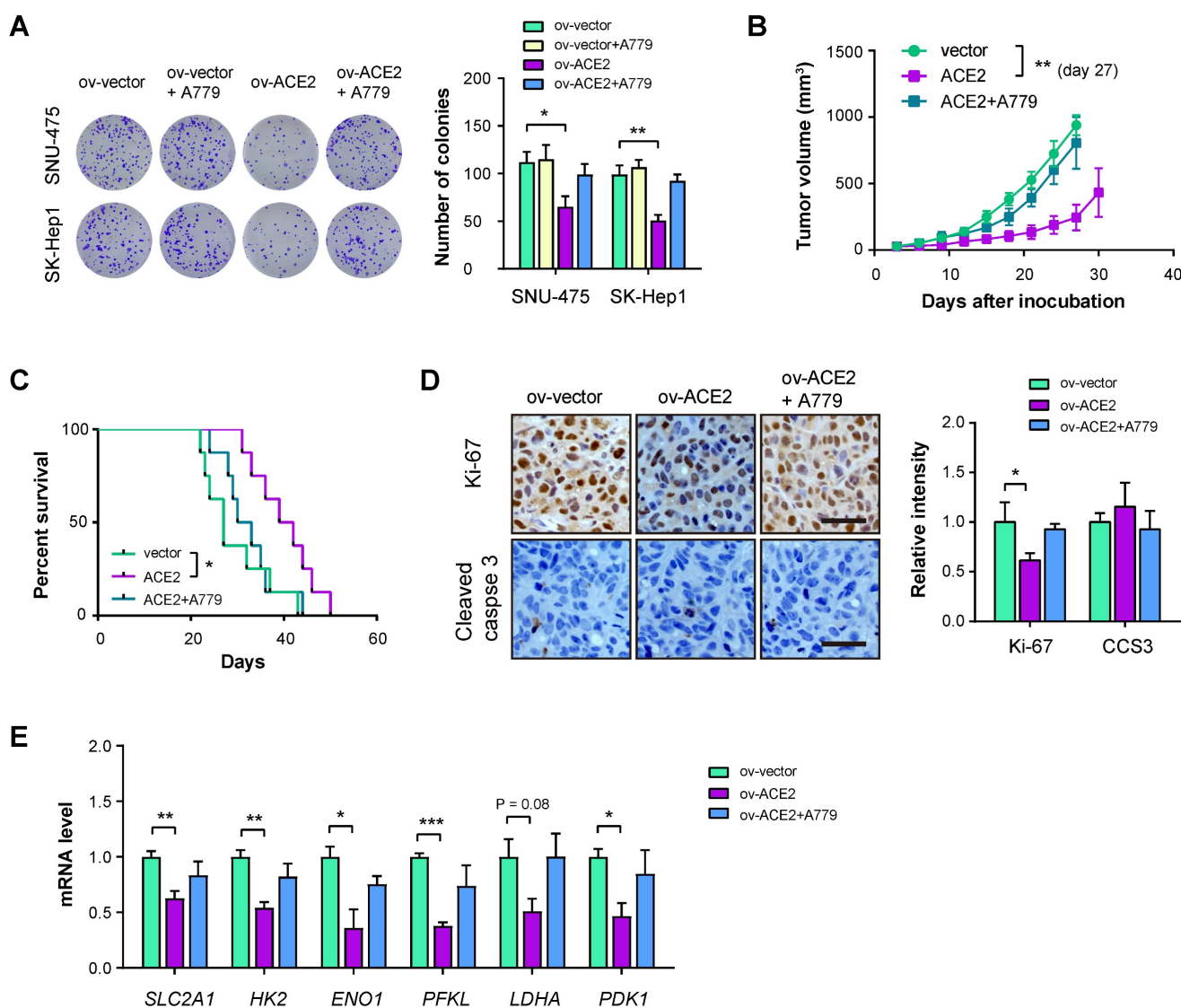


**Figure 5. ACE2 overexpression inhibits HCC tumor growth.** (A) The effects of ACE2 overexpression on *in vitro* proliferation of SNU-475 and SK-Hep1 cells in the presence or absence of A779 (1  $\mu$ M) were measured by colony formation assay (n = 3). (B) ov-vector and ov-ACE2 SK-Hep1 cells were subcutaneously injected into the nude mice (n = 5 per group) and tumor growth was monitored with or without A779 treatment. (C) Survival curve of mice in the ov-vector, ov-ACE2, and ov-ACE2 + A779 groups (n = 8 per group). (D) IHC analysis of Ki-67 and cleaved Caspase-3 (CCS3) in the tumor tissues from the ov-vector, ov-ACE2, and ov-ACE2 + A779 groups. Scale bar, 50  $\mu$ m. (E) qRT-PCR analysis of glycolytic components (SLC2A1, HK2, ENO1, PFKL, LDHA, and PDK1) in the tumor tissues from the ov-vector, ov-ACE2, and ov-ACE2 + A779 groups. Scale bar, 50  $\mu$ m. \*P < 0.05; \*\*P < 0.01; \*\*\*P < 0.001.

rapidly than tumors formed by sh-Ctrl HCC-LM3 cells (**Figure 6B**). Mice in the sh-ACE2-1 group had a lesser survival time compared with mice in the sh-Ctrl group (**Figure 6C**). The *in vivo* growth-promoting effects of ACE2 knockdown were also supported by Ki-67 staining (**Figure 6D**). Moreover, ACE2 knockdown increased the expression of glycolytic genes in xenograft tumor tissues (**Figure 6E**). Notably, both Ang-(1-7) and NAC can compromise the effects

of ACE2 knockdown on tumor growth and the expression of glycolytic components (**Figure 6A-E**). Notably, hijacking tumor glycolytic metabolism with the glycolysis inhibitor 2-DG largely abrogated the growth-promoting effects induced by ACE2 knockdown (**Supplementary Figure 5**). Collectively, these findings above indicate that ACE2 acts as a tumor suppressor in HCC.

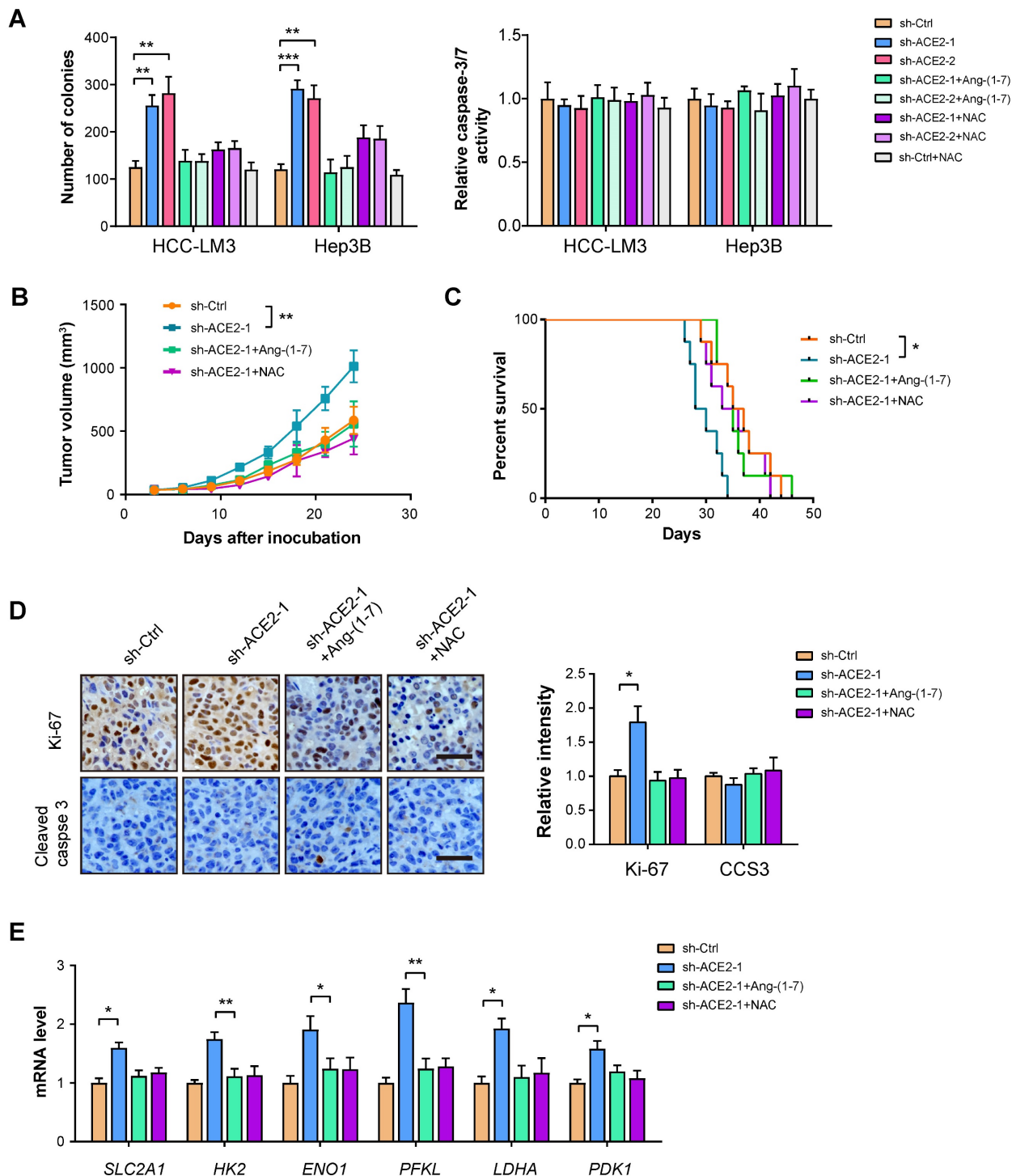


**Figure 6. ACE2 knockdown promotes HCC tumor growth.** (A) The effects of ACE2 knockdown on *in vitro* proliferation and apoptosis of HCC-LM3 and Hep3B cells in the presence or absence of Ang-(1-7) (10<sup>-8</sup> M) or NAC treatment (1 mM) were measured by colony formation assay and caspase-3/7 activity (n = 3), respectively. (B) sh-Ctrl and

sh-ACE2 HCC-LM3 cells were subcutaneously injected into the nude mice (n = 5 per group) and tumor growth was monitored with or without Ang-(1-7) or NAC treatment. (C) Survival curve of mice in the sh-Ctrl, sh-ACE2, sh-ACE2 + Ang-(1-7), and sh-ACE2 + NAC groups (n = 8 per group). (D) IHC analysis of Ki-67 and cleaved Caspase-3 (CCS3) in the tumor tissues from the sh-Ctrl, sh-ACE2, sh-ACE2 + Ang-(1-7), and sh-ACE2 + NAC groups; Scale bar, 50  $\mu$ m. (E) qRT-PCR analysis of glycolytic components (SLC2A1, HK2, ENO1, PFKL, LDHA, and PDK1) in the tumor tissues from the sh-Ctrl, sh-ACE2, sh-ACE2 + Ang-(1-7), and sh-ACE2 + NAC groups. \*P < 0.05; \*\*P < 0.01; \*\*\*P < 0.001.

### Clinical relevance of ACE2, p-SHP2, and HIF1 $\alpha$ in HCC samples

To add the clinical relevance, we first analyzed the protein expression of ACE2, phosphorylated-SHP2 (p-SHP2), and HIF1 $\alpha$  by IHC in a cohort of 202 HCC patients. Representative IHC images for ACE2, p-SHP2, and HIF1 $\alpha$  were shown in **Figure 7A**. As a result, a close and positive correlation between ACE2 and p-SHP2 was revealed (**Figure 7B**). In contrast, ACE2 expression was negatively associated with HIF1 $\alpha$  intensity (P < 0.001) in the HCC samples (**Figure 7C**). To test the therapeutic value of ACE2, we generated a patient-derived xenograft (PDX) model with two HCC samples, one sample with low ACE2 expression and one sample with high ACE2 expression (**Figure 7D**). As a result, xenografts from ACE2<sup>low</sup> tumors grew faster than ACE2<sup>high</sup> tumors. Interestingly, intratumoral injection of AAV-ovACE2 blocked the expression of ACE2<sup>low</sup> tumors (**Figure 7E**). Therefore, these results further confirm the ACE2-mediated molecular mechanism in the clinical setting.

### Discussion

Activation of oncogenes and inactivation of tumor suppressors are essential for the initiation and progression of HCC [9]. Ample evidence has deciphered the roles of oncogene-mediated metabolic reprogramming, however, limited knowledge is known about the underlying functional suppressor of aerobic glycolysis in HCC. In this study, we leveraged the molecular profile of HCC from the TCGA cohort and identified a series of DEGs that were negatively associated with aerobic glycolysis. Among them, ACE2 was demonstrated to exert its antitumor effect against HCC via generation of Ang-(1-7), which further acts on the G protein-coupled receptor Mas. Subsequently, pathway analysis revealed that p-SHP2/ROS/HIF1 $\alpha$  signaling was the downstream cascade of the ACE2/Ang-(1-7)/Mas receptor axis (**Figure 7F**).

In contrast to the actions of the ACE/Ang II/AT1 receptor, the ACE2/Ang-(1-7)/Mas receptor axis plays a counter-regulatory role on the same target, such as myocardium, blood vessels, brain, kidney, and other organs [43, 44]. In tumors, both positive and negative roles of ACE2 have been reported [23]. As shown in **Figure 1**, ACE2 expression was downregulated in most cancer types (BRCA, KICH, LIHC, PCPG, PRAD, and THCA), and upregulated ACE2 expression was observed at CESC,

ESCA, KIRP, LUAD, and UCEC. For the expression pattern of ACE2 in liver tissues, Hikmet et al. performed IHC analysis of ACE2 in a tissue microarray containing 18 cases of liver samples and showed that ACE2 was very low in hepatocytes [45]. In contrast, other studies revealed that ACE2 signals are expressed on hepatocytes, bile duct cells and liver endothelial cells [46]. In contrast, we revealed that ACE2 was variably expressed in non-tumor liver tissues though a large-scale sample investigation (n = 202). This discrepancy might be affected by multiple factors including but not limited to different cohort, the antibodies used and sample size detected. The role of ACE2 in cancers might be cancer-specific. Indeed, ACE2/Ang-(1-7)/Mas receptor has inhibitory effects on cancer cell proliferation in breast cancer, prostate cancer, and lung cancer [26, 47, 48], while Ang-(1-7) promotes cancer cell migration and invasion in human renal cell carcinoma [49]. In most cases, ACE2 is tumor-suppressive and acts as an inhibitor of tumor growth, metastasis, and angiogenesis. In alignment with previous report, we revealed that ACE2 is downregulated in HCC and higher ACE2 expression is associated with a better prognosis in HCC patients. Interestingly, we for the first time presented a previous unprecedented role of ACE2 in regulating aerobic glycolysis in HCC. Both *in vitro* and *in vivo* gain-of-function and loss-of-function studies supported the tumor suppressor function on aerobic glycolysis. Different from the situation in HCC, the ACE2/Ang-(1-7)/Mas receptor axis can enhance glucose uptake by skeletal muscle and inhibit hepatic gluconeogenesis [50], suggesting the context-dependent roles of ACE2.

The ACE2/Ang-(1-7)/Mas receptor can couple many intracellular signaling pathways to influence a range of actions under both physiology and disease stages [40]. In breast cancer, ACE2/Ang-(1-7)/Mas receptor axis inhibits the store-operated calcium entry and PAK1/NF- $\kappa$ B/Snail1 pathway [51]. However, we failed to notice significant changes in the NF- $\kappa$ B signal upon ACE2 overexpression in two HCC cell lines. ACE2/Ang-(1-7)/Mas receptor axis is also involved in the inhibition of MAPK signaling in diverse situations, such as inflammation and cancers [20, 41]. Interestingly, p-P38, p-ERK1/2, and p-JNK remained largely unaltered after ACE2 overexpression. Through pathway analyses and functional verification, we identified HIF1 $\alpha$  as a key change in response to ACE2 knockdown or overexpression.



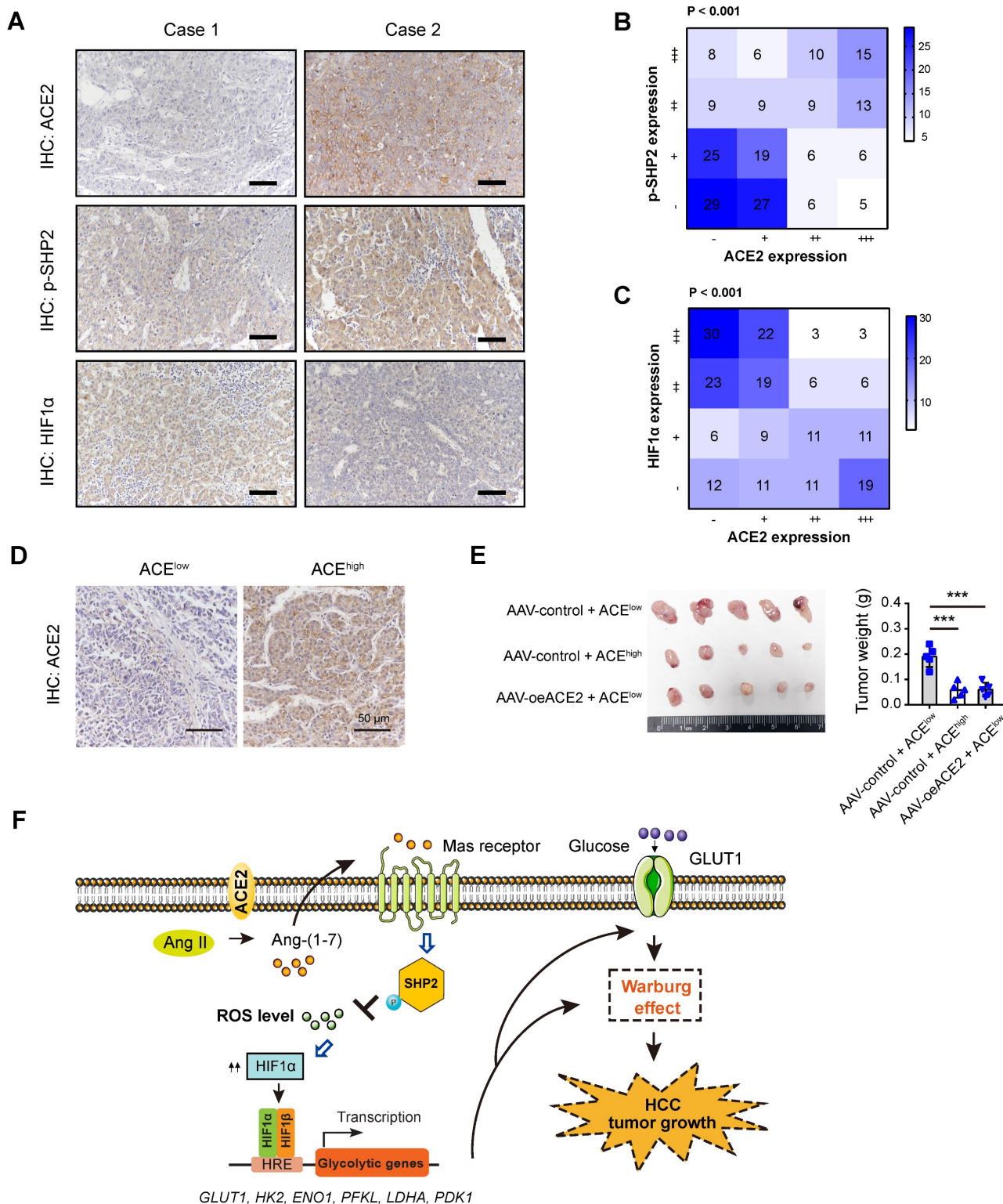


**Figure 7. Clinical relevance of ACE2 in HCC samples.** (A) Representative IHC staining of ACE2, HIF1α or p-SHP2 protein levels in human HCC specimens (n = 202); scale bar, 50 μm. (B) Correlation between ACE2 and p-SHP2 protein was determined by Spearman analysis. (C) Correlation between ACE2 and HIF1α protein was determined by Spearman analysis. (D) For PDX model, representative IHC staining of ACE2 in two HCC samples was shown. (E) The effect of ACE2 on the tumor growth of PDX xenograft was studied by a subcutaneous xenograft model. (F) The schematic diagram for the molecular mechanism of ACE2-mediated suppression of HIF1α activity and tumor growth in HCC. In brief, ACE2 metabolizes Ang II to Ang-(1-7), which activates Mas receptor and leads to the phosphorylation of SHP2. SHP2 activation blocks ROS generation, which further stabilizes HIF1α protein. HIF1α acts as a key transcriptional factor to induce the expression of glucose transporters and glycolytic genes and enhances the Warburg effect. Finally, tumor growth of HCC is suppressed by ACE2 due to compromised glycolytic flux. \*\*\*P < 0.001.

In line with our previous findings [18], intracellular ROS contributed to HIF1 $\alpha$  protein stabilization in HCC as blocking ROS with NAC suppressed HIF1 $\alpha$  activity. In human endothelial cells, Ang-(1-7) can counterregulate Ang II/AT1 receptor signaling to reduce ROS generation via the phosphorylation of SHP2 [42]. Consistently, genetic manipulation of ACE2 led to significant changes in the phosphorylated level of SHP2 in HCC cells. Therefore, we provided new insight regarding the molecular mechanism underlying the inhibitory role of the ACE2/Ang-(1-7)/Mas receptor axis in human cancers. Up to date, accumulating ACE2 agonists have been designed for many conditions, such as hypertension, myocardial Ischemia, type 2 diabetes mellitus, bone cancer, chondrosarcoma, and clear cell sarcoma of the kidney [27]. For instance, the antitrypanosomal agent diminazene aceturate (DIZE), an activator for ACE2, has been reported to play beneficial effects in several clinical models of hypertension, myocardial infarction, type 1 diabetes and atherosclerosis [52]. However, whether ACE2 activation are beneficial to cancer patients warrants further investigations. Since ACE inhibitors is widely used for cardiovascular diseases, our findings suggest that clinical use of ACE inhibitors may increase the incidence or the progression of HCC due to their potential roles in enhancing tumor glucose metabolism.

## Conclusions

Together, we identified ACE2 as a negative regulator against HCC glycolysis. Based on the background of aerobic glycolysis, activation of the ACE2/Ang-(1-7)/Mas receptor axis significantly retards tumor growth in HCC. Given that aberrant glucose metabolism is a general phenomenon in human solid cancers, targeting the ACE2/Ang-(1-7)/Mas receptor axis could be extended to other cancers. However, there are also several limitations in the present study. Firstly, effective assay is not developed to measure ACE2 activity in HCC cells and tumor tissues. Secondly, most of the data are acquired from *in vitro* cell experiments and *in vivo* nude mice, the implications of the ACE2/Ang-(1-7)/Mas receptor axis on the immune system are not studied.

## Abbreviations

HCC: hepatocellular carcinoma; ROS: reactive oxygen species; HIF1 $\alpha$ : hypoxia-inducible factor 1 $\alpha$ ; ECAR: extracellular acidification rate; NAC: N-acetylcysteine; ACE2: angiotensin converting enzyme 2; GSEA: gene set enrichment analysis; TCA: tricarboxylic acid cycle; ATP: adenosine triphosphate; TME: tumor microenvironment; GLUT1: glucose

transporter 1; HK2: hexokinase 2; PFKL: liver-type phosphofructokinase; LDHA: lactate dehydrogenase A; PKM2: pyruvate kinase M2; ccRCC: clear cell renal cell carcinoma; SARS-CoV-2: severe acute respiratory syndrome coronavirus 2; FDR: false discovery rate; BSA: bovine serum albumin; qRT-PCR: quantitative real-time PCR; LIHC: liver hepatocellular carcinoma.

## Supplementary Material

Supplementary figures and table.

<https://www.ijbs.com/v19p2613s1.pdf>

## Acknowledgements

The research was supported by grants from Shanghai Sailing Program (20YF1412000), National Key R&D Program of China (2018YFC2002000), National Natural Science Foundation of China (82001469 and 82071581), Shanghai Medical Leadership Training Program Grant (2019LJ09), Shanghai "Rising Stars of Medical Talents" Youth Development Program (Youth Medical Talents-Specialist Program), Shanghai Outstanding Young Medical Personnel Training Program (Excellence Project of Shanghai Municipal Health Commission, 20224Z0009), Xinxiu talents plan of Huadong Hospital (XXRC2210), and Key specialized diseases construction of Huadong Hospital (ZDZB2225).

## Availability of data and materials

All data generated or analyzed during this research are included in this manuscript.

## Author contributions

Zhijun Bao, Jie Chen, Shu-Heng Jiang and Xiaona Hu conceived the study plan and contributed to the revision of the final manuscript. Fangyuan Dong, Hui Li, Limin Liu, Jiaofeng Wang, Jianxia Ma, Gansheng Zhang and Jianfeng Yao performed the experiments, analyzed the data and finished the manuscript writing. Fangyuan Dong, Limin Liu, Lin-Li Yao, Shan Zhang, Jun Li and Shu-Heng Jiang contributed to the *in vitro* experiments. Fangyuan Dong and Limin Liu performed analysis and interpretation of data. All authors contributed to the writing and reviewing of the manuscript, and approved the final manuscript for submission.

## Consent for publication

We have obtained consent to publish from the participant to report individual patient data.

## Ethics approval and consent

All human samples were obtained with informed consent. All animals received humane care according to the criteria outlined in the "Guide for the Care and Use of Laboratory Animals" prepared by the

National Academy of Sciences and published by the National Institutes of Health.

## Competing Interests

The authors have declared that no competing interest exists.

## References

- Cairns RA, Harris IS, Mak TW. Regulation of cancer cell metabolism. *Nature reviews Cancer*. 2011; 11: 85-95.
- Orang AV, Petersen J, McKinnon RA, Michael MZ. Micromanaging aerobic respiration and glycolysis in cancer cells. *Mol Metab*. 2019; 23: 98-126.
- Vander Heiden MG, Cantley LC, Thompson CB. Understanding the Warburg effect: the metabolic requirements of cell proliferation. *Science*. 2009; 324: 1029-33.
- Hanahan D, Weinberg RA. Hallmarks of cancer: the next generation. *Cell*. 2011; 144: 646-74.
- Mu H, Yu G, Li H, Wang M, Cui Y, Zhang T, et al. Mild chronic hypoxia-induced HIF-2 $\alpha$  interacts with c-MYC through competition with HIF-1 $\alpha$  to induce hepatocellular carcinoma cell proliferation. *Cell Oncol (Dordr)*. 2021; 44: 1151-66.
- Cantor JR, Sabatini DM. Cancer cell metabolism: one hallmark, many faces. *Cancer discovery*. 2012; 2: 881-98.
- Feng Y, Xiong Y, Qiao T, Li X, Jia L, Han Y. Lactate dehydrogenase A: A key player in carcinogenesis and potential target in cancer therapy. *Cancer medicine*. 2018; 7: 6124-36.
- Schug ZT, Vande Voorde J, Gottlieb E. The Nurture of Tumors Can Drive Their Metabolic Phenotype. *Cell metabolism*. 2016; 23: 391-2.
- Feng J, Li J, Wu L, Yu Q, Ji J, Wu J, et al. Emerging roles and the regulation of aerobic glycolysis in hepatocellular carcinoma. *Journal of experimental & clinical cancer research : CR*. 2020; 39: 126.
- Dang CV. MYC on the path to cancer. *Cell*. 2012; 149: 22-35.
- Sukonina V, Ma H, Zhang W, Bartsaghi S, Subhash S, Heglind M, et al. FOXK1 and FOXK2 regulate aerobic glycolysis. *Nature*. 2019; 566: 279-83.
- Li L, Liang Y, Kang L, Liu Y, Gao S, Chen S, et al. Transcriptional Regulation of the Warburg Effect in Cancer by SIX1. *Cancer cell*. 2018; 33: 368-85 e7.
- Chen J, Zhang M, Ma Z, Yuan D, Zhu J, Tuo B, et al. Alteration and dysfunction of ion channels/transporters in a hypoxic microenvironment results in the development and progression of gastric cancer. *Cell Oncol (Dordr)*. 2021; 44: 739-49.
- Feng J, Dai W, Mao Y, Wu L, Li J, Chen K, et al. Simvastatin re-sensitizes hepatocellular carcinoma cells to sorafenib by inhibiting HIF-1 $\alpha$ /PPAR- $\gamma$ /PKM2-mediated glycolysis. *Journal of experimental & clinical cancer research : CR*. 2020; 39: 24.
- Luo X, Zheng E, Wei L, Zeng H, Qin H, Zhang X, et al. The fatty acid receptor CD36 promotes HCC progression through activating Src/PI3K/AKT axis-dependent aerobic glycolysis. *Cell death & disease*. 2021; 12: 328.
- Iansante V, Choy PM, Fung SW, Liu Y, Chai JG, Dyson J, et al. PARP14 promotes the Warburg effect in hepatocellular carcinoma by inhibiting JNK1-dependent PKM2 phosphorylation and activation. *Nature communications*. 2015; 6: 7882.
- Lin YH, Wu MH, Huang YH, Yeh CT, Cheng ML, Chi HC, et al. Taurine up-regulated gene 1 functions as a master regulator to coordinate glycolysis and metastasis in hepatocellular carcinoma. *Hepatology*. 2018; 67: 188-203.
- Dong F, Li R, Wang J, Zhang Y, Yao J, Jiang SH, et al. Hypoxia-dependent expression of MAP17 coordinates the Warburg effect to tumor growth in hepatocellular carcinoma. *Journal of experimental & clinical cancer research : CR*. 2021; 40: 121.
- Scialo F, Daniele A, Amato F, Pastore L, Matera MG, Cazzola M, et al. ACE2: The Major Cell Entry Receptor for SARS-CoV-2. *Lung*. 2020; 198: 867-77.
- Simoes e Silva AC, Silveira KD, Ferreira AJ, Teixeira MM. ACE2, angiotensin-(1-7) and Mas receptor axis in inflammation and fibrosis. *Br J Pharmacol*. 2013; 169: 477-92.
- Rodrigues Prestes TR, Rocha NP, Miranda AS, Teixeira AL, Simoes ESAC. The Anti-Inflammatory Potential of ACE2/Angiotensin-(1-7)/Mas Receptor Axis: Evidence from Basic and Clinical Research. *Curr Drug Targets*. 2017; 18: 1301-13.
- Patel VB, Zhong JC, Grant MB, Oudit GY. Role of the ACE2/Angiotensin 1-7 Axis of the Renin-Angiotensin System in Heart Failure. *Circ Res*. 2016; 118: 1313-26.
- Xu J, Fan J, Wu F, Huang Q, Guo M, Lv Z, et al. The ACE2/Angiotensin-(1-7)/Mas Receptor Axis: Pleiotropic Roles in Cancer. *Front Physiol*. 2017; 8: 276.
- Murphy KT, Hossain MI, Swiderski K, Chee A, Naim T, Trieu J, et al. Mas Receptor Activation Slows Tumor Growth and Attenuates Muscle Wasting in Cancer. *Cancer research*. 2019; 79: 706-19.
- Geng YL, Ding YJ, Ni L, Xu KD, Le VM, Ji R, et al. The role of angiotensin-(1-7) on acquired platinum resistance-induced angiogenesis in non-small cell lung cancer in vitro and in vivo. *Neoplasma*. 2021; 68: 770-9.
- Zhang Q, Lu S, Li T, Yu L, Zhang Y, Zeng H, et al. ACE2 inhibits breast cancer angiogenesis via suppressing the VEGFa/VEGFR2/ERK pathway. *Journal of experimental & clinical cancer research : CR*. 2019; 38: 173.
- Khanna P, Soh HJ, Chen CH, Saxena R, Amin S, Naughton M, et al. ACE2 abrogates tumor resistance to VEGFR inhibitors suggesting angiotensin-(1-7) as a therapy for clear cell renal cell carcinoma. *Sci Transl Med*. 2021; 13.
- Dong F, Yang Q, Wu Z, Hu X, Shi D, Feng M, et al. Identification of survival-related predictors in hepatocellular carcinoma through integrated genomic, transcriptomic, and proteomic analyses. *Biomedicine & pharmacotherapy = Biomedecine & pharmacotherapie*. 2019; 114: 108856.
- Jiang SH, Zhu LL, Zhang M, Li RK, Yang Q, Yan JY, et al. GABRP regulates chemokine signalling, macrophage recruitment and tumour progression in pancreatic cancer through tuning KCNN4-mediated Ca(2+) signalling in a GABA-independent manner. *Gut*. 2019; 68: 1994-2006.
- Jiang SH, Li J, Dong FY, Yang JY, Liu DJ, Yang XM, et al. Increased Serotonin Signaling Contributes to the Warburg Effect in Pancreatic Tumor Cells Under Metabolic Stress and Promotes Growth of Pancreatic Tumors in Mice. *Gastroenterology*. 2017; 153: 277-91 e19.
- Lu C, Fang S, Weng Q, Lv X, Meng M, Zhu J, et al. Integrated analysis reveals critical glycolytic regulators in hepatocellular carcinoma. *Cell Commun Signal*. 2020; 18: 97.
- Xiao Y, Yang K, Liu P, Ma D, Lei P, Liu Q. Deoxyribonuclease 1-like 3 Inhibits Hepatocellular Carcinoma Progression by Inducing Apoptosis and Reprogramming Glucose Metabolism. *Int J Biol Sci*. 2022; 18: 82-95.
- Herraez E, Lozano E, Macias RI, Vaquero J, Bujanda L, Banales JM, et al. Expression of SLC22A1 variants may affect the response of hepatocellular carcinoma and cholangiocarcinoma to sorafenib. *Hepatology*. 2013; 58: 1065-73.
- Quiroga AD, Ceballos MP, Parody JP, Comanzo CG, Lorenzetti F, Pisani GB, et al. Hepatic carboxylesterase 3 (Ces3/Tgh) is downregulated in the early stages of liver cancer development in the rat. *Biochimica et biophysica acta*. 2016; 1862: 2043-53.
- Zhu M, Xu W, Wei C, Huang J, Xu J, Zhang Y, et al. CCL14 serves as a novel prognostic factor and tumor suppressor of HCC by modulating cell cycle and promoting apoptosis. *Cell death & disease*. 2019; 10: 796.
- Chen SL, Zhang CZ, Liu LL, Lu SX, Pan YH, Wang CH, et al. A GYS2/p53 Negative Feedback Loop Restricts Tumor Growth in HBV-Related Hepatocellular Carcinoma. *Cancer research*. 2019; 79: 534-45.
- Wei RR, Zhang MY, Rao HL, Pu HY, Zhang HZ, Wang HY. Identification of ADH4 as a novel and potential prognostic marker in hepatocellular carcinoma. *Med Oncol*. 2012; 29: 2737-43.
- Liu J, Li W, Zhao H. CFHR3 is a potential novel biomarker for hepatocellular carcinoma. *Journal of cellular biochemistry*. 2020; 121: 2970-80.
- Heffelfinger SC, Hawkins HH, Barrish J, Taylor L, Darlington GJ. SK HEP-1: a human cell line of endothelial origin. *In Vitro Cell Dev Biol*. 1992; 28A: 136-42.
- Kong Y, Zhao X, Qiu M, Lin Y, Feng P, Li S, et al. Tubular mas receptor mediates lipid-induced kidney injury. *Cell death & disease*. 2021; 12: 110.
- Santos RAS, Sampaio WO, Alzamora AC, Motta-Santos D, Alenina N, Bader M, et al. The ACE2/Angiotensin-(1-7)/MAS Axis of the Renin-Angiotensin System: Focus on Angiotensin-(1-7). *Physiol Rev*. 2018; 98: 505-53.
- Sampaio WO, Henrique de Castro C, Santos RA, Schiffrin EL, Touyz RM. Angiotensin-(1-7) counterregulates angiotensin II signaling in human endothelial cells. *Hypertension*. 2007; 50: 1093-8.
- Bader M. ACE2, angiotensin-(1-7), and Mas: the other side of the coin. *Pflugers Arch*. 2013; 465: 79-85.
- Pinheiro SV, Simoes ESAC. Angiotensin converting enzyme 2, Angiotensin-(1-7), and receptor MAS axis in the kidney. *Int J Hypertens*. 2012; 2012: 414128.



45. Hikmet F, Mear L, Edvinsson A, Micke P, Uhlen M, Lindskog C. The protein expression profile of ACE2 in human tissues. *Molecular systems biology*. 2020; 16: e9610.
46. Lei HY, Ding YH, Nie K, Dong YM, Xu JH, Yang ML, et al. Potential effects of SARS-CoV-2 on the gastrointestinal tract and liver. *Biomedicine & pharmacotherapy = Biomedecine & pharmacotherapie*. 2021; 133: 111064.
47. Soto-Pantoja DR, Menon J, Gallagher PE, Tallant EA. Angiotensin-(1-7) inhibits tumor angiogenesis in human lung cancer xenografts with a reduction in vascular endothelial growth factor. *Molecular cancer therapeutics*. 2009; 8: 1676-83.
48. Krishnan B, Torti FM, Gallagher PE, Tallant EA. Angiotensin-(1-7) reduces proliferation and angiogenesis of human prostate cancer xenografts with a decrease in angiogenic factors and an increase in sFlt-1. *Prostate*. 2013; 73: 60-70.
49. Zheng S, Yang Y, Song R, Yang X, Liu H, Ma Q, et al. Ang-(1-7) promotes the migration and invasion of human renal cell carcinoma cells via Mas-mediated AKT signaling pathway. *Biochemical and biophysical research communications*. 2015; 460: 333-40.
50. Zhao S, Sun W, Jiang P. Role of the ACE2/Ang-(1-7)/Mas axis in glucose metabolism. *Rev Cardiovasc Med*. 2021; 22: 769-77.
51. Yu C, Tang W, Wang Y, Shen Q, Wang B, Cai C, et al. Downregulation of ACE2/Ang-(1-7)/Mas axis promotes breast cancer metastasis by enhancing store-operated calcium entry. *Cancer letters*. 2016; 376: 268-77.
52. Qaradakhi T, Gadanec LK, McSweeney KR, Tacey A, Apostolopoulos V, Levinger I, et al. The potential actions of angiotensin-converting enzyme II (ACE2) activator diminazene aceturate (DIZE) in various diseases. *Clin Exp Pharmacol Physiol*. 2020; 47: 751-8.